Turbulent Flow of Non-Newtonian Systems

D. W. DODGE and A. B. METZNER

University of Delaware, Newark, Delaware

A theoretical analysis for turbulent flow of non-Newtonian fluids through smooth round tubes has been performed for the first time and has yielded a completely new concept of the attending relationship between the pressure loss and mean flow rate. In addition, the analysis has permitted the prediction of non-Newtonian turbulent velocity profiles, a topic on which the published literature is entirely silent.

To confirm the theoretical analysis, experimental data were taken on both polymeric gels and solid-liquid suspensions under turbulent-flow conditions. Fluid systems with flow-behavior indexes between 0.3 and 1.0 were studied at Reynolds numbers as high as 36,000. All the fully turbulent experimental data supported the validity of the theoretical analysis. The final resistance-law correlation represents a generalization of von Karman's equation for Newtonian fluids in turbulent flow and is applicable to all non-Newtonians for which the shear rate depends only on shear stress, irrespective of rheological classification. All the turbulent experimental data for the non-Newtonian systems were correlated by this _____ship with a mean deviation of 1.9%.

THEORY

Non-Newtonian fluids are defined as materials which do not conform to a direct proportionality between shear stress and shear rate. Because of this negative definition of non-Newtonian behavior, essentially an infinite number of possible rheological relationships exist for this class of fluids, and as yet no single equation has been proved to describe exactly the shear-stress–shear-rate relationships of all such materials over all ranges of shear rates. If such a general equation could be developed, it seems probable that its complexity would be too great for general engineering utility. Although it is desirable that the following theoretical analysis be universally applicable to all time-dependent, nonelastic fluids, irrespective of any arbitrary rheological classifications such as *Bingham plastic, pseudoplastic,* or *dilatant,* this consideration is much too broad to be handled in the initial phases of the development. Therefore a particular rheological model will be selected for use initially, and application of the resulting development to fluids deviating from the assumed model will be considered subsequently.

It has been found experimentally (*7, 11, 19, 20*) that the relationship between shear stress and shear rate for a great many non-Newtonian fluids, possibly the majority, may be represented closely over wide ranges of shear rate (ten- to one-thousand-fold) by a two-constant power function of the form

$$\tau = K\left(\frac{-du}{dr}\right)^n \qquad (1)$$

where $(-du/dr)$ is the shear rate written for flow within a circular duct. An equation of this type, though empirical, appears to represent the rheological properties for a wide variety of non-Newtonian fluids better than most other proposed equations and certainly better than any other available two-constant equation. For this reason the power-law rheological model will be adopted in the following theoretical analysis. It should be noted that the power-law model includes the special case of Newtonian behavior, namely that case when n is unity and K is equal to the Newtonian viscosity. Values of n between zero and unity characterize pseudoplastic fluids, for which the apparent viscosity [defined by $\tau/(-du/dr)$] decreases with increasing shear rate. Conversely values of n greater than unity correspond to dilatant fluids, for which the apparent viscosity increases with shear rate. Generally it may be said that n is an index to the degree of non-Newtonian behavior in that the further n is removed from unity, above or below, the more pronounced become the non-Newtonian characteristics. On the other hand, K is related more to the consistency of the system (*9, 10*).

Power-Law Fluids

Resistance Law

The general method of attack to be used here is similar to that first employed by Millikan (*12*) for Newtonian fluids. However an additional degree of freedom represented by the flow-behavior index will be incorporated into the analysis.

According to a concept which has been used successfully with Newtonian fluids, flow in a smooth pipe may be divided into the following three zones:

1. A laminar sublayer lying next to the pipe wall in which the effects of turbulence are negligible
2. A transition zone in which the effects of turbulence and viscous shear are of the same order of magnitude
3. A turbulent core comprising the bulk of the fluid stream. Here the momentum transfer which accompanies the random velocity fluctuations characteristic of turbulent motion, rather than viscous shear, determines the velocity profile. If one assumes the turbulent fluctuations to be independent of viscosity, it follows that the effects of viscosity are negligible in the turbulent core. It will be assumed that the same type of flow division is applicable to non-Newtonian fluids. When one defines y as the distance of a point within the pipe from the tube wall, the extent of the flow zones will be designated as

$$\text{laminar sublayer: } 0 \leqq y \leqq \delta$$

$$\text{transition zone: } \delta \leqq y \leqq \lambda$$

$$\text{turbulent core: } \lambda \leqq y \leqq R$$

For Newtonian fluids it has been shown (*5*) that the time average velocity at a point within a smooth pipe depends on five independent variables, R, ρ, τ_w, μ, and y. With non-Newtonian fluids of the power-law type the two flow parameters n and K are required to

D. W. Dodge is with E. I. DuPont de Nemours and Company, Inc., Buffalo, New York.

replace the single rheological proportionality constant for Newtonian systems. By analogy to the Newtonian case then it is reasonable to assume that for power-law fluids.

$$u = f(R, \rho, \tau_w, K, n, y) \qquad (2)$$

When one applies dimensional analysis, Equation (2) may be written as

$$\frac{u}{u^*} = f_1(Z, \xi, n) \qquad (3)$$

where

$$Z = R^n \rho (u^*)^{2-n}/K \qquad (4)$$

In the derivation of Equation (3), no assumptions were made regarding the location of the point corresponding to u, and therefore the equation is valid for all values of y or ξ.

Within the laminar sublayer the pipe radius plays no part in determining u. The effect of R therefore might be assumed negligible also at slightly greater distances from the wall, as far out as the outer part of the turbulent core. Then within this wall region

$$u = f(\rho, \tau_w, K, n, y)$$

which according to dimensional analysis may be expressed as

$$\frac{u}{u^*} = f_2(Z\xi^n, n) \qquad (5)$$

Equation (5) is comparable with Prandtl's wall-velocity law (*5*) for Newtonian fluids, which agrees well with experimental results. It shall be assumed that this equation is valid in the range $0 \leqq \xi \leqq \xi_1$, where ξ_1 is only slightly greater than λ/R. It is not meant to be implied that the function f_2 will have the same specific form in the laminar sublayer and in the outer part of the turbulent core; generally the forms will be different.

The difference between the velocity at the center line of a tube and the time average velocity at a point elsewhere within the turbulent core has been called the *velocity defect*. From Equation (2) it can be seen that this defect $(U_m - u)$ depends at most on R, ρ, τ_w, K, n, and y. However in the core $(U_m - u)$ will be determined by the random turbulent fluctuations which have been assumed independent of the apparent viscosity. This assumption has been substantiated for Newtonian fluids. For power-law systems the equivalent assumption is that the velocity defect is independent of K (but not of n), whereby

$$U_m - u = f(\tau_w, \rho, R, y, n)$$

Application of dimensional analysis here yields

$$\frac{U_m - u}{u^*} = f_3(\xi, n) \qquad (6)$$

When n is unity, Equation (6) becomes what is commonly called the *velocity-defect law* for Newtonian fluids, which also has been amply verified by experiments (*5*).

Equation (6) is strictly applicable only in the turbulent core, that is for $\lambda/R \leqq \xi \leqq 1$. If as an approximation one were to assume that Equation (6) applies over the entire cross section, then it follows that

$$V = \frac{2}{R^2}\int_0^R ur\,dr$$

$$= \frac{2}{R^2}\int_0^R U_m r\,dr - \frac{2u^*}{R^2}\int_0^R f_3(\xi, n) r\,dr$$

For any specified value of n this equation becomes

$$V = U_m - u^* \quad \text{(constant)}$$

or

$$\frac{U_m - V}{u^*} = P_n \qquad (7)$$

Since Equation (7) was derived for any fixed value of n, it must be expected in general that P_n will be a function of n. Experiments with Newtonian fluids have shown that the wall layers are so thin that Equation (7) may be used without appreciable error; it will be assumed that the same is true for the non-Newtonian case. This assumption should be very good for pseudoplastic fluids $(0 < n < 1)$ for which a laminar sublayer even thinner than that in the Newtonian case is to be expected, but it may break down for fluids having a value of n sufficiently above unity to retain an appreciable thickness of the laminar sublayer even under fully turbulent conditions.

The friction factor is defined by

$$f = \tau_w \Big/ \frac{\rho V^2}{2} = \frac{D\Delta P}{4L} \Big/ \frac{\rho V^2}{2}$$

Therefore

$$\frac{V}{u^*} = \sqrt{\frac{2}{f}} \qquad (8)$$

When one writes Equation (3) for the center line of the pipe,

$$\frac{U_m}{u^*} = f_1(Z, 1, n) = F_1(Z, n) \qquad (9)$$

by a combination of Equations (7), (8), and (9)

$$\sqrt{\frac{2}{f}} = F_1(Z, n) - P_n \qquad (10)$$

Hence an expression for the friction factor may be obtained by finding $F_1(Z, n)$.

In the outer part of the turbulent core, where $(\lambda/R) \leqq \xi \leqq \xi_1$, Equations (5) and (6) are both assumed to be valid. Therefore eliminating u/u^* from Equations (5) and (6) and replacing U_m/u^* by Equation (9), one finds for this overlapping region

$$f_2(Z\xi^n, n) = F_1(Z, n) - f_3(\xi, n)$$

It will be noted that ξ effects the left side of this equation according to ξ^n, and that the F_1 function on the right side is independent of ξ. To balance the left side of the equation ξ must be present in the f_3 function also as ξ^n rather than ξ. Hence this equation may be formulated better as

$$f_2(Z\xi^n, n) = F_1(Z, n) - f_3(\xi^n, n) \qquad (11)$$

If n is now eliminated as a variable by considering any fixed value of n, Equation (11) becomes

$$f_{2n}(Z\xi^n) = F_{1n}(Z) - f_{3n}(\xi^n) \qquad (12)$$

When one lets

$$\frac{df_{2n}}{d(Z\xi^n)} = f_{2n}'$$

then

$$\left(\frac{\partial f_{2n}}{\partial Z}\right)_\xi \quad \frac{df_{2n}}{d(Z\xi^n)}\left(\frac{\partial(Z\xi^n)}{\partial Z}\right)_\xi = f_{2n}'\xi^n$$

and by Equation (12)

$$f_{2n}'\xi^n = \frac{dF_{1n}}{dZ} \qquad (13)$$

Similarly

$$\left(\frac{\partial f_{2n}}{\partial \xi^n}\right)_Z = \frac{df_{2n}}{d(Z\xi^n)}\left(\frac{\partial(Z\xi^n)}{\partial \xi^n}\right)_Z = f_{2n}'Z$$

and by Equation (12)

$$f_{2n}'Z = -\frac{df_{3n}}{d\xi^n} \qquad (14)$$

From Equation (13) it is seen that f_{2n}' must have the form $f(Z)/\xi^n$, since dF_{1n}/dZ is independent of ξ. Furthermore from Equation (14) it is seen that f_{2n}' must have the form $f(\xi^n)/Z$, since $df_{3n}/d\xi^n$ is independent of Z. Both these requirements can be satisfied only if

$$f_{2n}' = \frac{A_n}{Z\xi^n} \qquad (15)$$

Now by Equations (13) and (15)

$$dF_{1n}(Z) = A_n \frac{dZ}{Z}$$

whereby

$$F_{1n}(Z) = \left(\frac{U_m}{u^*}\right) = A_n \ln Z + B_n \qquad (16)$$

By Equations (14) and (15)

$$df_{3n}(\xi^n) = -A_n \frac{d\xi^n}{\xi^n}$$

whereby

$$f_{3n}(\xi^n) = \left(\frac{U_m - u}{u^*}\right) = -A_n \ln \xi^n + E_n \quad (17)$$

The constants of integration in Equations (16) and (17) must be considered as functions of n unless later proved otherwise. When one combines Equations (12), (16), and (17),

$$f_{2n}(Z\xi^n) = \frac{u}{u^*} = A_n \ln Z\xi^n + B_n - E_n \quad (18)$$

The derivation of Equations (16), (17), and (18) was based on a consideration of the overlapping region $\lambda/R \leqq \xi \leqq \xi_1$, wherein Equations (5) and (6) were equated. As a result it should be expected that these equations can be applied rigorously only to this region. However Equation (16) is independent of ξ and hence must be truly independent of the location and width of the overlapping region. This can also be seen from the definition of $F_1(Z, n)$ as given by Equation (9); its applicability cannot be limited to a particular region of ξ. Considering the original statement of the velocity-defect law, Equation (6), one may modify Equation (17) for all values of ξ within the turbulent core

$$\frac{U_m - u}{u^*} = -nA_n \ln \xi + g_1(\xi, n) \quad (19)$$

where $g_1(\xi, n)$ is some unknown function. Equation (19) extends the region of applicability of Equation (17) to the entire turbulent core simply by making it more general. An alternate equation for the velocity profile, valid for the entire turbulent core but not including U_m, may be formulated from Equations (16) and (19):

$$\frac{u}{u^*} = \frac{U_m}{u^*} - \frac{U_m - u}{u^*} = A_n \ln Z\xi^n + B_n - g_1(\xi, n) \quad (20)$$

If Equation (16) is now substituted into Equation (10), one obtains

$$\sqrt{\frac{2}{f}} = A_n \ln Z + B_n - P_n$$

which by suitable manipulation together with Equations (4) and (8) can be put in the form (3)

$$\sqrt{\frac{1}{f}} = A_{1n} \log [N_{Re}{}^0 (f)^{1-n/2}] + C_n \quad (21)$$

where

$$N_{Re}{}^0 = D^n V^{2-n} \rho / K \quad (22)$$

$$A_{1n} = 1.628 A_n$$

$$C_n = 0.4901 A_n \left(1 + \frac{n}{2}\right) + B_n - P_n$$

$N_{Re}{}^0$ is not so convenient a Reynolds number for correlation purposes as one proposed by Metzner and Reed (11), the reason being that the use of $N_{Re}{}^0$ does not result in a unique relationship between the friction factor and the Reynolds number in the laminar-flow region. Instead a family of curves result with n as a parameter. The generalized Reynolds number of Metzner and Reed, $N_{Re}{}'$, however does result in a unique relationship in the laminar region for all values of n, namely the familiar laminar relationship $f = 16/N_{Re}{}'$. The work of Metzner and Reed was based on concepts developed initially by Rabinowitsch (13), who clearly established the fact that for laminar flow through a round tube of any fluid with a shear rate that is a function only of shear stress the relationship between the shear stress at the tube wall $D\Delta P/4L$ and the quantity $8V/D$ is unique. Hence the flow characteristics of a fluid are defined just as completely by the laminar $D\Delta P/4L - 8V/D$ relationship as by the shear-stress-shear-rate relationship, and for pipe-flow situations the former is generally more convenient (10).

In their work Metzner and Reed used the following definitions to define the laminar-flow behavior of non-Newtonian fluids. (These definitions were then used under turbulent-flow conditions as well, just as the viscosity of a Newtonian fluid is defined under laminar conditions but used in both the laminar and turbulent regions.)

$$n' = \frac{d(\log (D\Delta P/4L))}{d(\log (8V/D))} \quad (23)$$

$$\tau_w = \frac{D\Delta P}{4L} = K'(8V/D)^{n'} \quad (24)$$

Equation (23) defines n', and Equation (24) defines K'. Generally Equation (24) does not represent an integration of Equation (23); only when n' is a constant are the two definitions linked by a simple integration. It will be noted that a marked similarity exists between Equations (1) and (24). The power-law case represents the one situation where n' and K' are true constants and are related to the parameters n and K by the equations (9, 11)

$$n' = n \quad (25)$$

$$K' = K\left(\frac{3n + 1}{4n}\right)^n \quad (26)$$

Hence with constant values of n' and K' Equation (24) is simply another statement of the power-law model applied to flow in round tubes.

By use of Equations (25) and (26) it can be shown that for power-law fluids $N_{Re}{}^0$ and $N_{Re}{}'$ are related by

$$N_{Re}{}^0 = \frac{1}{8}\left(\frac{6n' + 2}{n'}\right)^{n'} N_{Re}{}' \quad (27)$$

where

$$N_{Re}{}' = \frac{D^{n'} V^{2-n'} \rho}{g_c K' (8)^{n'-1}} \quad (28)$$

Inspection shows that both $N_{Re}{}^0$ and $N_{Re}{}'$ reduce to the conventional Reynolds number $DV\rho/\mu$ for the Newtonian case ($n = n' = 1$). If one replaces $N_{Re}{}^0$ by $N_{Re}{}'$, Equation (21) becomes

$$\sqrt{\frac{1}{f}} = A_{1n} \log [N_{Re}{}' (f)^{1-n'/2}] + C_n' \quad (29)$$

where

$$C_n' = A_{1n} \log \left[\left(\frac{1}{8}\right)\left(\frac{6n' + 2}{n'}\right)^{n'}\right] + C_n$$

Equation (29) is the goal which has been sought. Here the form of the equation relating the friction factor and the Reynolds number has been found for the turbulent flow of power-law fluids in a smooth round pipe. It remains for A_{1n} and C_n', two unknown functions of n', to be determined experimentally. Two special cases are of particular interest, namely the Newtonian case ($n' = 1$) and the case of ultimate pseudoplasticity ($n' = 0$).

Newtonian Case

If Equation (29) is valid as postulated, it should hold for the Newtonian case where n' is unity. For this situation the equation reduces to

$$\sqrt{\frac{1}{f}} = A \log \left[\frac{DV\rho}{\mu} \sqrt{f}\right] + C$$

A resistance law of this type was proposed first by von Karman (18) and subsequently by Prandtl (14), both of whom arrived at their conclusion from mixing-length theories. Newtonian data obtained by Nikuradse agreed extremely well with such a relationship and led to the final formula (5, 6, 15)

$$\sqrt{\frac{1}{f}} = 4.0 \log \left[\frac{DV\rho}{\mu} \sqrt{f}\right] - 0.40 \quad (30)$$

Hence for the Newtonian case ($n' = 1$)

$$A_{1n}(1) = 4.0$$

$$C_n'(1) = -0.40$$

It would appear that the von Karman equation, Equation (30), represents a special case of the more general equation derived here for use with Newtonian and non-Newtonian fluids alike.

Ultimate Pseudoplastic Case

Velocity profiles may readily be analyzed mathematically for laminar flow of power-law fluids. Typical laminar-velocity-profile plots for several values of n' have been presented by Metzner (9), reproductions of which are shown in

Figure 1. For Newtonian fluids in laminar flow the velocity profile is parabolic. As n' decreases toward zero, the laminar-velocity profile becomes progressively flatter, and in the limiting case of $n' = 0$ it is perfectly flat. On passing from the laminar- to the turbulent-flow region the laminar-velocity profile is flattened by a net turbulent momentum transfer from the high- to the low-velocity areas. Hence turbulence leads to the same general effect on the velocity profile as does a decreasing value of n'. Further, for when n' is close to zero, the laminar-velocity profile is so nearly flat that it can be altered only very little on passing from laminar to turbulent flow. In the limiting case of $n' = 0$, where the laminar profile is perfectly flat, there can be no distinction between laminar- and turbulent-velocity profiles. The separate friction-factor correlations normally encountered for Newtonian fluids for the laminar- and turbulent-flow regions arise from the change in the relationship between the wall shear rate and the mean velocity, that is the change in the velocity profile which occurs on passing from laminar to turbulent conditions. As the difference between the laminar and turbulent profiles diminishes, so must the difference between the laminar and turbulent friction-factor relationships. In the limit where the two profiles are identical, as represented by the case $n' = 0$, the laminar and turbulent friction-factor–Reynolds-number relationships become the same. The same conclusion may also be reached by noting that the apparent viscosity of this fluid is infinite a short distance from the wall, suppressing the turbulence completely. Therefore the turbulent curve for the case of $n' = 0$ is simply an extension of the laminar-flow line

$$f = 16/N_{Re}' \qquad (31)$$

According to Equation (29) a plot of $\sqrt{1/f}$ vs. log $[N_{Re}'(f)^{1-n'/2}]$ at a given value of n' should be a straight line of slope A_{1n}. When $n' = 0$,

$$\log [N_{Re}'(f)^{1-n'/2}] = \log [N_{Re}'f] = \log 16$$

Thus a plot of $\sqrt{1/f}$ vs. log $[N_{Re}'(f)^{1-n'/2}]$ will be a straight line of infinite slope, whereby it is concluded that for an n' of zero $A_{1n}(0) = \infty$. When one considers C_n' as an intercept, it is further concluded that $C_n'(0) = -\infty$.

Turbulent-Velocity Profiles

In addition to the results regarding turbulent friction factors the preceding analysis has yielded some significant information about turbulent velocity profiles for non-Newtonian fluids. It has been predicted that turbulent profiles for power-law fluids may be expressed by Equations (19) or (20), both of which are valid for the entire turbulent core and hence for almost all the fluid stream

$$\frac{U_m - u}{u^*} = -n' A_n \ln \xi + g_1(\xi, n') \qquad (19)$$

$$\frac{u}{u^*} = A_n \ln Z\xi^{n'} + B_n - g_1(\xi, n') \qquad (20)$$

Before use can be made of these equations, however, it is necessary to appraise the function $g_1(\xi, n')$.

First one must consider the turbulent Newtonian case for which the following equations of Prandtl are commonly

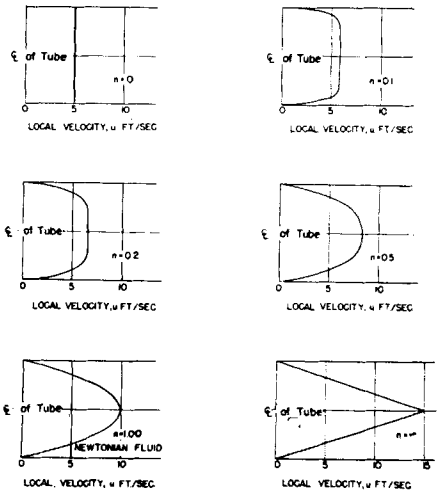

Fig. 1. Laminar velocity profiles for power-law fluids.

accepted as *universal velocity distribution laws (15)*

$$\frac{U_m - u}{u^*} = -\frac{1}{k} \ln \xi \qquad (32)$$

$$\frac{u}{u^*} = \frac{1}{k} \ln Z\xi + B \qquad (33)$$

Comparison of Equations (32) and (33) with Equations (19) and (20) shows that the Newtonian equations may be considered as special cases of Equations (19) and (20), where $A_n(1) = 1/k$ and $g_1(\xi, 1) = 0$. Actually these Newtonian equations cannot be exact, since they do not predict a zero slope of the velocity profile at the center line. Hence although the $g_1(\xi, 1)$ function must be zero at the center line itself, it cannot be precisely zero in the immediate neighborhood thereof. However this discrepancy is so slight and localized that Prandtl's equations represent the experimental data very well, and it can be concluded that the assumption of $g_1(\xi, 1) = 0$ is an excellent approximation.

Other limits or boundary conditions may also be placed on the g_1 function. Since the turbulent-velocity profile for fluids with an n' of zero is perfectly flat, it is required that $g_1(\xi, 0) = 0$. Furthermore at the center line of the tube $\xi = 1$ the velocity defect is zero for all values of n' by definition, and so $g_1(1, n') = 0$. Finally, the preceding analysis showed that in the region $\lambda/R \leqq \xi \leqq \xi_1$, g_1 is independent of ξ and is a function of n' at most. Here g_1 is equal to the integration constant E_n of Equation (17), which could also be zero.

In view of the several known situations where g_1 is equal to zero, it would appear that at least a reasonable approximation of turbulent-velocity profiles for power-law fluids could be obtained by assuming $g_1(\xi, n') = 0$. Therefore subsequent predictions of turbulent-velocity profiles will be based on the assumption that the g_1 function is zero, whereby

$$\frac{U_m - u}{u^*} = -n' A_n \ln \xi = -1.415 n' A_{1n} \log \xi \qquad (34)$$

$$\frac{u}{u^*} = A_n \ln Z\xi^{n'} + B_n \qquad (35)$$

Although such predictions should be considered as approximate at the present time, they represent the first bit of information available in this area and should prove to be of considerable value. Determination of the validity of the assumption regarding the g_1 function must await experimental measurements of non-Newtonian turbulent-velocity profiles.

Equations for the turbulent-velocity profiles of Newtonian systems are frequently expressed in terms of dimensionless parameters. When one modifies and expands these definitions to include all power-law fluids, Equation (35) becomes

$$u^+ = A_n \ln y^+ + B_n \qquad (36)$$

where

$$u^+ = u/u^* \qquad (37)$$

$$y^+ = Z\xi^n = y^n(u^*)^{2-n}\rho/K \qquad (38)$$

These new proposed definitions for u^+ and y^+ reduce to the familiar interpretation for the special case of Newtonian behavior.

Equation (36), like Equations (34) and (35), is assumed to hold throughout the turbulent core only. The laminar sublayer on the other hand is assumed sufficiently thin that the shear stress may be considered constant therein and equal to τ_w. Within the laminar sublayer, then, the velocity varies linearly with y, and

$$\tau = \tau_w = K\left(\frac{-du}{dr}\right)_w^n = K\left(\frac{u}{y}\right)^n$$

which may be rearranged as

$$u^+ = (y^+)^{1/n} \qquad (39)$$

Again the usual Newtonian equation of $u^+ = y^+$ for the laminar sublayer (*5*) is simply a special case of the more general expression given by Equation (39).

Analysis of Unknown Functions

Since no detailed picture of the actual physical mechanism of turbulence was used in the preceding developments, the theory is not capable of giving complete results. It should be emphasized, however, that this same situation exists at the present time even for the simpler case of turbulent Newtonian flow.

The primary functions of greatest importance here are A_{1n} and C_n'. The other functions encountered, namely A_n, B_n, C_n, and P_n, can be related to these. Some such relationships have already been indicated. The function P_n came about by integration of the general velocity-defect law. Now that a functional form has been proposed for this law, it is possible to evaluate P_n further. When one employs Equation (34) as the f_3 function, the earlier integration leads to

$$P_n = \frac{U_m - V}{u^*} = \frac{3}{2} n' A_n$$

$$= \frac{3}{2}\left(\frac{n' A_{1n}}{1.628}\right) \qquad (40)$$

The functions A_n, B_n, C_n, and P_n now have all been related to the primary functions A_{1n} and C_n'.

Two special cases regarding A_{1n} and C_n' have already been mentioned, namely

$$A_{1n}(1) = 4.0 \quad C_n'(1) = -0.40$$

$$A_{1n}(0) = \infty \quad C_n'(0) = -\infty$$

Little more can be said about C_n' prior to experimental investigation. Several facts concerning A_{1n}, however, can be established initially. Examining Equation (34) one obviously first observes that A_{1n} can never be negative, since the velocity defect is always positive and $\log \xi$ is always negative (or zero). Second the velocity defect should become zero at all ξ for limiting case of $n' = 0$, whereby it is concluded that

$$\lim_{n' \to 0} (n' A_{1n}) = 0$$

despite the fact that $A_{1n}(0) = \infty$. Apparently A_{1n} approaches infinity more slowly than n' approaches zero. At the other extreme the velocity defect must remain bounded as n' increases without limit, a situation that leads to the conclusion

$$\lim_{n' \to \infty} (A_{1n}) = 0$$

Laminar-velocity profiles for power-law fluids are illustrated in Figure 1. Here it is shown that as n' decreases toward zero the velocity profile becomes progressively flatter. All the corresponding turbulent-velocity profiles for finite values of n' will be considerably flatter owing to the equalizing effect of turbulent momentum transfer. If it is further assumed that this flattening effect does not pass through any maximum or minimum point as n' decreases toward zero, the turbulent velocity defect at a given ξ, and hence the product $n'A_{1n}$, will decrease with decreasing n' values. After the known Newtonian point has been selected as a reference, it is possible to place the following restrictions on the A_{1n} function:

$$A_{1n} < 4.0/n' \quad \text{for} \quad n' < 1$$

$$A_{1n} > 4.0/n' \quad \text{for} \quad n' > 1$$

Nonpower-Law Fluids

The developments of the preceding sections have been based on the assumption that the laminar relationship between shear stress and shear rate for the fluid under consideration can be represented by a simple power function. For nonpower-law fluids the property parameters n and K or n' and K' may still be employed, but in this case they are functions of the shear stress rather than than true constants. The parameters have meaning here only when associated with a specific shear stress.

In a discussion of nonpower-law fluids one fact should be emphasized. The fluid behavior is of interest only in the range of actual shear stresses present in a given flow situation. For a fluid flowing in a pipe or circular duct the shear stress acting on the fluid varies linearly with the radius from zero at the center line to a maximum value given by $D\Delta P/4L$ at the pipe wall. Hence for a particular flow situation it is entirely irrelevant if the fluid deviates from the power-law behavior only at shear stresses which are higher than this maximum at the pipe wall.

Nonpower-law fluids pose no problem in laminar-flow situations. It has been shown (*10, 11*) that the laminar relationship $f = 16/N_{Re}'$ is rigorously valid regardless of whether or not n' and K' are constant. When the fluid-property parameters are functions of the shear stress, it is necessary simply to evaluate them at the existing wall shear stress. For turbulent flow the problem on nonconstant fluid property parameters is more complex. However Equation (29) can be validated for the nonpower-law case, if it is possible to select values of the fluid-property parameters such that the equation still defines the relationship between the wall shear stress and the mean velocity. Hence for the nonpower-law case the problem becomes one of establishing the shear stress at which the fluid-property parameters should be evaluated to avoid or at least minimize any error in the wall shear-rate–mean-velocity relationship. The following analysis is performed in an attempt to find values of the parameters which, when used in Equation (29), will represent a good approximation to the actual, but mathematically more complex, flow situation.

Figure 2 shows a typical Newtonian turbulent-velocity profile (water flowing through a 1-in. pipe at a Reynolds number of 20,000). It will be noted that in the region near the center line the Newtonian profile is quite flat; that is (du/dr) is very small. Furthermore, according to earlier reasoning, as n' approaches zero, the velocity profile becomes progressively flatter. This fact indicates that for pseudoplastics at least the mean velocity is relatively insensitive to any variations in n' in the low shear-stress regions near the center of the tube; in contrast the mean velocity is highly dependent on the high-shear-rate regions near the wall.

To develop this quantitatively one may consider the contribution of the various shear-rate regions to the mean velocity. The contribution of the differential slice illustrated in Figure 2 to the volumetric flow rate is given by

$$dQ = \pi r^2 \, du$$

This incremental contribution to the volumetric flow rate is attributable to the shear rate occurring at r and as such is a measure of the dependence of the mean velocity on the shear rate occurring at a shear stress of $\tau_w(r/R)$. When one normalizes this point contribution and integrates,

$$\frac{\Delta Q}{Q} = \frac{\Delta V}{V} = \frac{\int_u^{U_m} r^2 \, du}{\int_0^{U_m} r^2 \, du}$$

$\Delta V/V$ represents the fraction of V which would be unaccounted for if the velocity profile were cut off perfectly flat from radius all the way to the center line. Figure 3 is a plot of the fractional-flow contribution $\Delta V/V$ as a function of r/R or (τ/τ_w) based on the turbulent Newtonian velocity profile given in Figure 2. Figure 3 dramatically shows that the mean velocity is highly dependent on the shear rates in the very close proximity of the wall and is essentially independent of the shear rates nearer to the center of the tube. For example Figure 3 shows that the shear rates occurring at an r/R or τ/τ_w less than 0.8 account for only 7% of the mean velocity. Therefore any variation in n at shear stresses less than $0.8\tau_w$ would cause an error in only this 7% contribution to the mean velocity. Since the 7% represents the fraction of the mean velocity that would be unaccounted for if the velocity

profile were cut off perfectly flat for all r/R less than 0.8, a situation far worse than can be anticipated as due to any reasonable variation in n', the error in the mean velocity due to a variation of the flow-behavior index in this region would be only a small fraction of this 7% and entirely negligible. On the other hand about 74% of the mean-flow contribution is attributable to the shear rates which occur at shear stresses between τ_w and $0.96\tau_w$.

These observations lead inescapably to the conclusion that Equation (29) is an excellent approximation for predicting the friction factor for nonpower-law fluids, provided the parameters are evaluated at the existing wall shear stress. Since the turbulent velocity profiles for many pseudoplastic fluids should be flatter than for the Newtonian

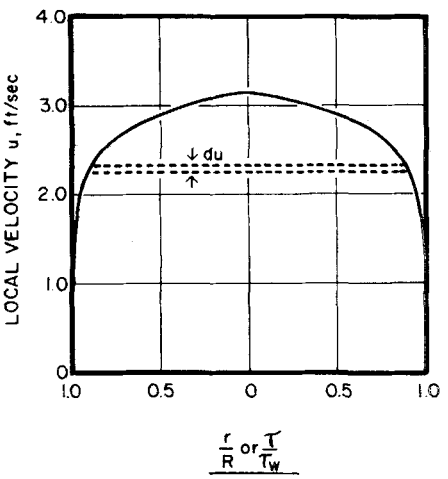

Fig. 2. Newtonian turbulent velocity distribution

(N_{Re} = 20,000, D = 1 in., water at 20°C.).

case developed here, the situation depicted by Figure 3 should be even more dramatic in this case. For the limiting case of $n' = 0$ Figure 3 would be simply two straight lines coinciding with the coordinate axes. Conversely the situation will be less pronounced for dilatant fluids. However even in the dilatant case the mean velocity will be dependent most highly on the wall shear rate, and the same conclusions will probably be valid in most practical cases.

It has now been shown that the friction-factor relationships for both laminar and turbulent flow as given by Equations (31) and (29) respectively are valid for nonpower-law fluids, provided the fluid-property parameters are evaluated at the existing wall shear stress. Unfortunately the wall shear stress is normally the quantity being sought, and hence a trial-and-error procedure is necessitated when one is working with nonpower-law fluids. Equation (29) would be used repeatedly to calculate the pressure drop until the calculated τ_w was identical to the shear stress at which n' and K' were evaluated. It should be emphasized, however, that the majority of non-Newtonian fluids can be represented quite well by the power-law model and that the remaining fluids seldom depart radically from this model. Thus in most cases there is a reasonably large region surrounding the existing wall shear stress in which n' and K' are nearly constant, and the convergence of the trial-and-error procedure is rapid. A further increase in the rapidity of convergence is provided by the manner in which n' and K' change together with shear stress. If the fluid-property parameters vary at all with shear stress, they must vary in opposite directions. For example if n' increases with increasing shear stress, then K' must decrease with increasing τ. Such a combination of variations tends to cancel their effect on N_{Re}', leaving the Reynolds number only weakly dependent on the shear stress at which the parameters are evaluated.

All this discussion has been aimed at extending the power-law friction-factor prediction to include nonpower-law fluids. It is also important to be able to extend the power-law results regarding turbulent-velocity profiles to nonpower-law systems. This should be possible, at least approximately, in the sense that velocity profiles for nonpower-law fluids might be constructed differentially on the basis of the power-law results. The differential form of the velocity-defect law, if no contribution by a g_1 function is assumed, is given by

$$d\left(\frac{U_m - u}{u^*}\right) = -nA_n \frac{d\xi}{\xi}$$

Thus the slope of the velocity-defect plot is a function of n and ξ. For power-law fluids (nA_n) is a constant independent of ξ, and this equation may be integrated directly to give Equation (34), the velocity-defect law for power-law fluids. With nonpower-law fluids (nA_n) will be a function of the shear stress and hence of ξ. When one denotes (nA_n) by $f(\xi)$, the velocity-defect law for nonpower-law fluids may be written as

$$\frac{U_m - u}{u^*} = \int_1^{\xi} -f(\xi)\frac{d\xi}{\xi}$$

Assumption of Strict Similarity

If in place of the velocity-defect law as given by Equation (6), an assumption of strict similarity is made, that is

$$\frac{u}{U_m} = f_3^s(\xi, n)$$

one obtains the following equations as the most important results from an analysis similar to that presented here on the basis of the power-law model (*3*):

$$\frac{u}{U_m} = \xi^{n'e_n} \tag{41}$$

$$f = \frac{a_n}{(N_{Re}')^{b_n}} \tag{42}$$

$$b_n = \frac{2e_n}{1 + e_n(2 - n')}$$

Equations (41) and (42) are of the same form as the Blasius equations for Newtonian fluids (*6*). In this case the numerical values of a_n, b_n, and e_n respectively are approximately 0.079, 0.25, and 1/7 for Reynolds numbers between 10^4 and 10^5.

Although the friction-factor correlation suggested by Equation (42) is inferior to

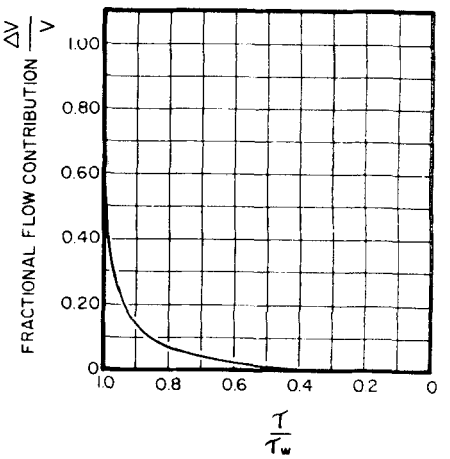

Fig. 3. Newtonian fractional flow contribution

$$\frac{\Delta V}{V} = \frac{\int_u^{U_m} r^2\, du}{\int_0^{U_m} r^2\, du}$$

that of Equation (29), the former has the advantage of expressing the friction factor explicitly. For certain applications, such as the development of heat and mass transfer analogies, this advantage may well overshadow the accompanying sacrifice in precision, as it has for Newtonian fluids, and result in the practical utilization of Equation (42). The attractiveness of such an approximation is perhaps even more important with non-Newtonian systems.

EXPERIMENTAL

The purpose of the experimental phase of this investigation was to test the validity of the proposed theoretical developments and, if found valid, to evaluate the unknown functions A_{1n} and C_n' which occur therein. The primary criteria for selection of experimental fluids were that they exhibit a wide range of non-Newtonian characteristics

under the turbulent experimental conditions. Also it was desirable that fluids representative of both polymeric solutions and solid-liquid suspensions be investigated. Finally the validity of the theoretical analysis could could best be tested by considering non-power-law as well as power-law fluids. Owing to the viscosity characteristics of dilatant systems and the attending difficulties which arise in handling these fluids under conditions of high shear, the experimental systems were restricted to pseudoplastic fluids. In view of the far greater industrial importance of pseudoplastic fluids in comparison with dilatant systems, this restriction does not constitute a serious limitation.

Aqueous solutions of Carbopol 934 and sodium carboxymethycellulose served to represent polymeric solutions, while slurries of Attasol, an attapulgite clay, represented the class of solid-liquid suspensions. Four concentrations of Carbopol, three of Attasol, and two of carboxymethycellulose (CMC) were studied. In addition, data were taken with two Newtonian fluids, water and a sugar solution, to test the equipment and experimental technique.

Fluid was pumped from an agitated storage tank through one of three horizontal test sections, after which the fluid was recycled. The flow rate was measured either by timing a sample collected in a weigh tank or by a Foxboro magnetic flowmeter installed in the recycle line. Test sections of ½-, 1-, and 2-in. (nominal) smooth brass pipe were employed. Calming or entrance lengths of about 53 pipe diam. preceded the first pressure tap for each test section, and exit lengths greater than 12 pipe diam. followed the last pressure tap before any type of geometric discontinuity was encountered. Pressure taps were formed by small holes carefully drilled through the pipe walls and rounded slightly on the inside by means of a fine file to remove any burs. To verify uniformity of the pressure gradient each test section was divided evenly into subsections, the ½- and 1-in. pipes having three subsections constituting their test sections and the 2-in. pipe having two. The pressure drop could be measured across any of these subsections individually or across the whole of the test sections. To establish further that the pressure-gradient measurements were free from the abnormalities which prevail near an entrance, three pressure taps were located within the calming section of the ½-in. pipe. With these it was intended to trace the entrance effects and verify their dissipation prior to the entry of the test sections. Water was used as the pressure-transmitting medium in the lines connecting the pressure taps to the manometers. Bourdon gauges and two sets of manometers employing fluids of different densities provided pressure-drop measurements over a wide range (0.02 to 160 lb./sq. in.). For each test fluid a few points were taken in the laminar-flow region to check the rheological data and to permit establishment of the point of turbulence inception. After each change in flow rate the manometer lines were flushed clean of any material that had worked its way into them by movement of the manometer legs.

A capillary-tube viscometer, equipped with a constant-temperature bath and suitable for measurements at shear rates in excess of $(10)^5$ sec.$^{-1}$, was used to establish rheological properties of the fluids under investigation. Viscometric data were normally taken with two different capillary tubes, all of which were first calibrated with National Bureau of Standards' oils. Rheological measurements were made before and after a pipeline run, with special attention being paid to the shear-stress region that was encountered during the pipeline experiments. A detailed description of the apparatus and experimental procedure is available (*3*).

Typical viscometric data for one of the test fluids are shown in Figure 4. Only two of the non-Newtonian fluids studied truly conformed to the power-law model over the entire range of shear stresses wherein measurements were made. Several additional fluids however approached power-law behavior very closely within restricted regions of shear stress. Generally the polymeric solutions tended more toward power-law behavior than did the clay suspensions.

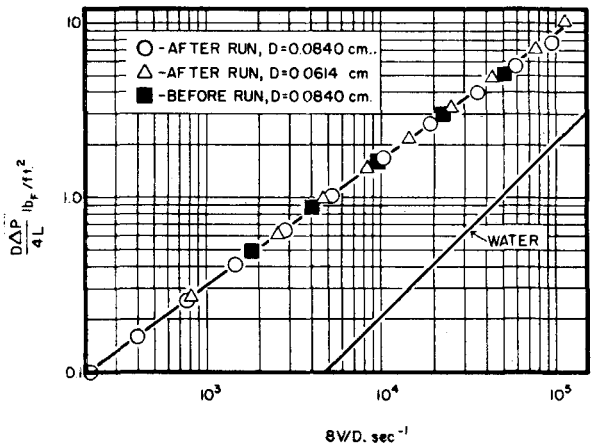

Fig. 4. Flow curve for 0.2% carbopol.

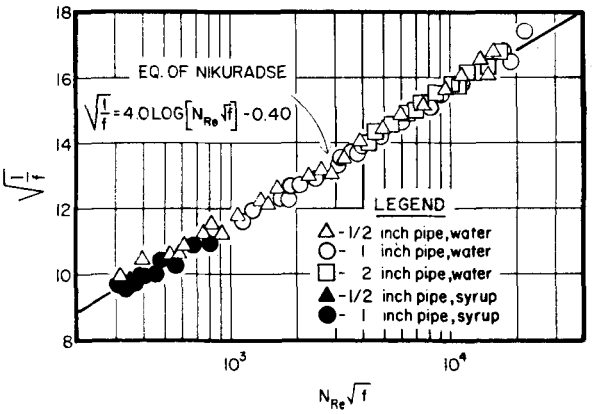

Fig. 6. Turbulent Newtonian data, correlation variables.

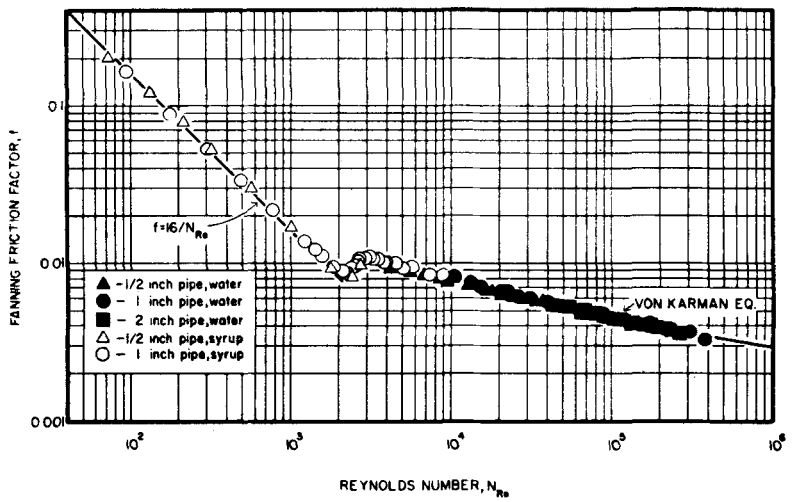

Fig. 5. Friction factor plot of Newtonian data used to check experimental accuracy.

Results

The experimental Newtonian results relating the friction factor and Reynolds number are plotted in Figure 5 in the form of a conventional friction-factor diagram. This figure shows that the Newtonian data of this investigation are in excellent agreement with the

established Newtonian relationships for all three flow regions, laminar, transition, and turbulent. Hence it was concluded that the equipment and techniques used in this study were entirely satisfactory, yielding accurate and reliable data. The turbulent Newtonian data are plotted in Figure 6 in terms of the correlating groups of the von Karman equation $\sqrt{1/f}$ and log $[N_{Re}\sqrt{f}]$. Again the good agreement between the data and the established relationship is evident.

Experimental data taken with the non-Newtonian systems covered the range of variables outlined approximately in Table 1. Figure 7 shows friction-factor data typical of the experimental results for these non-Newtonian systems. Perhaps the most striking feature about Figure 7 is that the turbulent friction-factor data lie below the Newtonian curve and above an extension of the laminar relationship. From the discussions regarding the special cases of Newtonian and ultimate pseudoplastic behavior, it is to be expected that friction factors for all pseudoplastic systems will fall within this general region. Hence, qualitatively at least, Figure 7 supports the earlier theoretical considerations. Second, the friction-factor diagram clearly shows a definite transition region between laminar and turbulent flow which extends over a range of Reynolds numbers comparable to the extent of the Newtonian transition region. According to Figure 7 the onset of turbulence occurred at a Reynolds number slightly larger than the accepted Newtonian value of 2,100.

To test the validity of the theoretically predicted friction-factor correlation, plots of $\sqrt{1/f}$ vs. log $[N_{Re}'(f)^{1-n'/2}]$ are much more informative than the ordinary friction-factor diagrams shown in Figure 7. Figure 8 shows the turbulent data of Figure 7 plotted in terms of the correlation variables. It is evident that the points do fall on a straight line as predicted, the slope being A_{1n}. Because of the requirement that n' be constant throughout the range of experimental measurements, this test could be applied only to the power-law portion of the present data. Of the non-Newtonian fluids tested, four agreed sufficiently well with the power-law model to permit evaluation of the A_{1n} function in this manner.

The theoretical considerations that A_{1n} approaches infinity as n' goes to zero and approaches zero as n' goes to infinity suggest that a logarithmic plot of A_{1n} vs. n' might be fruitful in determining the form of the A_{1n} function. Figure 9 is such a logarithmic plot showing all the experimental points of the A_{1n} function. Although a single correlating line was indicated in Figure 8 for the data at an n' of 0.726, it will be noted that separate and slightly different values of A_{1n} are shown in Figure 9 at this flow-behavior index for each of the three pipe diameters. The individual values of A_{1n} here were established by the separate consideration of the data obtained from each of the different pipes and application of least-square techniques thereto. Similarly, by fitting separate least-squares lines through the Newtonian data of Figure 6 for each of the three pipes, slightly different values of A_{1n} (1) were obtained. It was not the purpose of the present Newtonian data to test the validity of the von Karman equation and its coefficients. Rather it is accepted herein that the coefficients of Equation (30) are reliable for the Newtonian case. However for purposes of comparison with the non-Newtonian measurements it was informative to perform this evaluation of A_{1n} (1) independently based on the present Newtonian data. Since it is well established for Newtonian fluids that no extraneous diameter effects exist, it is concluded that the indicated non-Newtonian diameter discrepancies in A_{1n} do not constitute a real effect.

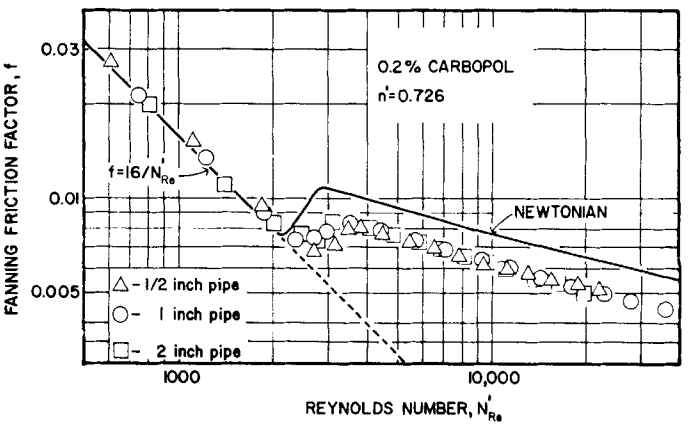

Fig. 7. Typical non-Newtonian friction factor results.

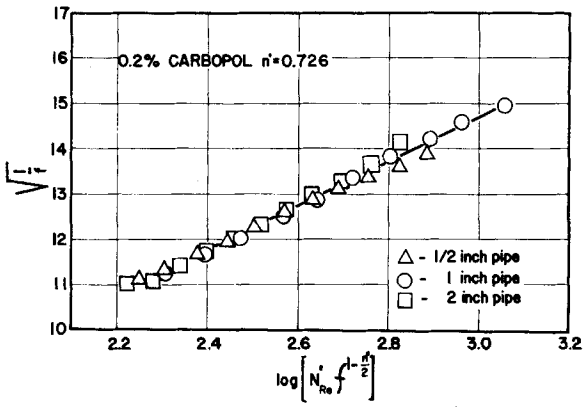

Fig. 8. Turbulent data from Figure 7 plotted in terms of the correlation variables.

Table 1. Range of Experimental Variables for Non-Newtonian Systems

Fluid	N_{Re}' Range	n' Range	point values of n' (in 1 in. pipe) N_{Re}': 5,000	10,000	20,000
0.5% Carbopol	670 - 6,000	0.43-0.56	0.54		
0.4% Carbopol	720-11,000	0.51-0.58	0.54	0.57	
0.3% Carbopol	750-19,000	0.62	0.62	0.62	
0.2% Carbopol	610-36,000	0.73	0.73	0.73	0.73
15 % Attasol	540-11,000	0.28-0.44	0.38	0.43	
13 % Attasol	740-22,000	0.26-0.57	0.42	0.49	0.56
11.8% Attasol	830-21,000	0.22-0.68	0.40	0.60	0.68

Generally the experimental data for the 1-in. pipe covered a wider range of the correlation variables from which A_{1n} was determined, and therefore the results for this pipe probably represent better values than for the other two pipes. The line shown in Figure 9 passing through the data was determined by the method of least squares after placing on it the requirement that it must pass through the point $A_{1n}(1) = 4.0$. The equation of this line is given by

$$A_{1n} = \frac{4.0}{(n')^{.75}} \qquad (43)$$

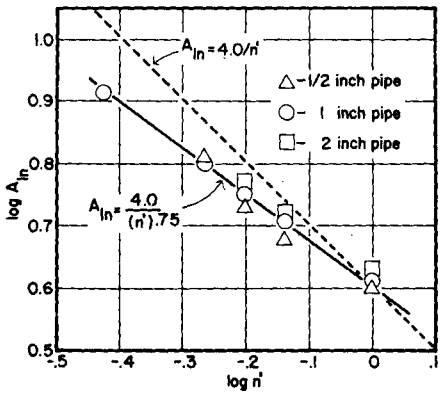

Fig. 9. The A_{1n} function: variance with the flow behavior index n'.

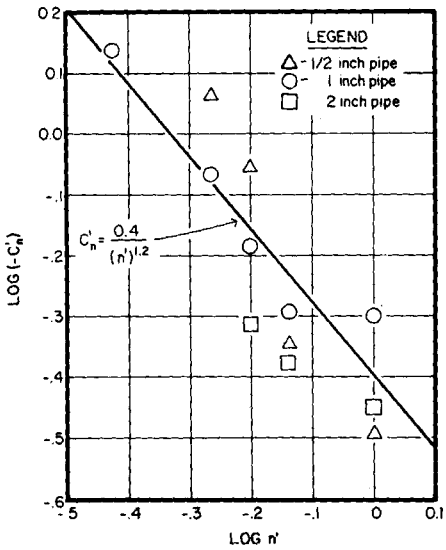

Fig. 10. Dependence of the C_n' function on n'.

Besides passing through the known Newtonian point, the expression proposed for the A_{1n} function satisfies all the theoretical restrictions discussed earlier, namely,

$$A_{1n}(n') \gtrless 0$$

$$A_{1n}(0) = \infty$$

$$A_{1n}(\infty) = 0$$

$$n'A_{1n}(0) = 0$$

$$A_{1n} < 4.0/n' \quad (\text{for } n' < 1.0)$$

$$A_{1n} > 4.0/n' \quad (\text{for } n' > 1.0)$$

Hence although the proposed A_{1n} function must be considered as empirical, it is entirely compatible with all the known theoretical prerequisites.

The C_n' results calculated by using the A_{1n} values given by Equation (43) are shown in Figure 10. The wide scatter of the data shown here can be attributed to the inaccuracies encountered in determining C_n', a small number, by the subtraction of one large number from another. Although such an operation makes it difficult to obtain accurate values of C_n', it should be remembered that by the same token the relationship between the friction factor and Reynolds number is quite insensitive to the C_n' function. Hence a high degree of precision is not required in this quantity for the purpose of pressure-loss prediction, at least in the n' range investigated here. Again, the discrepancies between data for the various pipe sizes are about the same for both the Newtonian and non-Newtonian points. Also the differences are not consistent in their direction, and it is concluded that no real additional diameter effect exists.

There is no justification at the present time for placing anything other than a straight line through the data points of Figure 10. The line shown in this figure was located by the method of least squares by incorporating the requirement that it pass through the accepted Newtonian point $C_n'(1) = -0.40$. The equation of this line is

$$C_n' = \frac{-0.40}{(n')^{1.2}} \qquad (44)$$

Equation (46) satisfies the Newtonian situation and the one theoretical condition imposed upon C_n' earlier, namely that C_n' approach negative infinity as n' goes to zero.

The final proposed friction-factor correlation is obtained by replacing the general functions A_{1n} and C_n' of Equation (29) with their specific forms as given by Equations (43) and (44) respectively.

$$\sqrt{\frac{1}{f}} = \frac{4.0}{(n')^{.75}} \log\left[N_{Re}'(f)^{1-n'/2}\right] - \frac{0.40}{(n')^{1.2}} \qquad (45)$$

The A_{1n} and C_n' functions and Equation (45) were established by using only that portion of the experimental data corresponding to power-law fluids or very close approximations thereof. It is difficult to test the compliance of the data for nonpower-law fluids with the theoretical hypotheses. For example, nonpower-law data cannot be tested by a plot such as Figure 8, since the flow-behavior index is not constant. Even presentation of these data in terms of the familiar friction-factor diagram is of little significance because of the changing values of n' with Reynolds numbers. Further, if the flow-behavior index is a function of shear stress, its value at a given Reynolds number will be different for the three pipe sizes, and the friction-factor data for the various pipe diameters would not even coincide. Earlier it was predicted that Equation

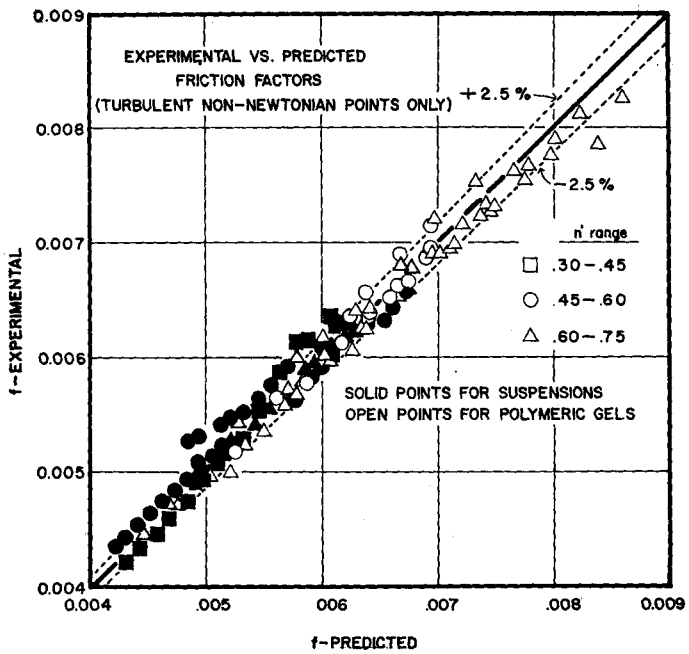

Fig. 11. Comparison of experimental friction factors with those predicted.

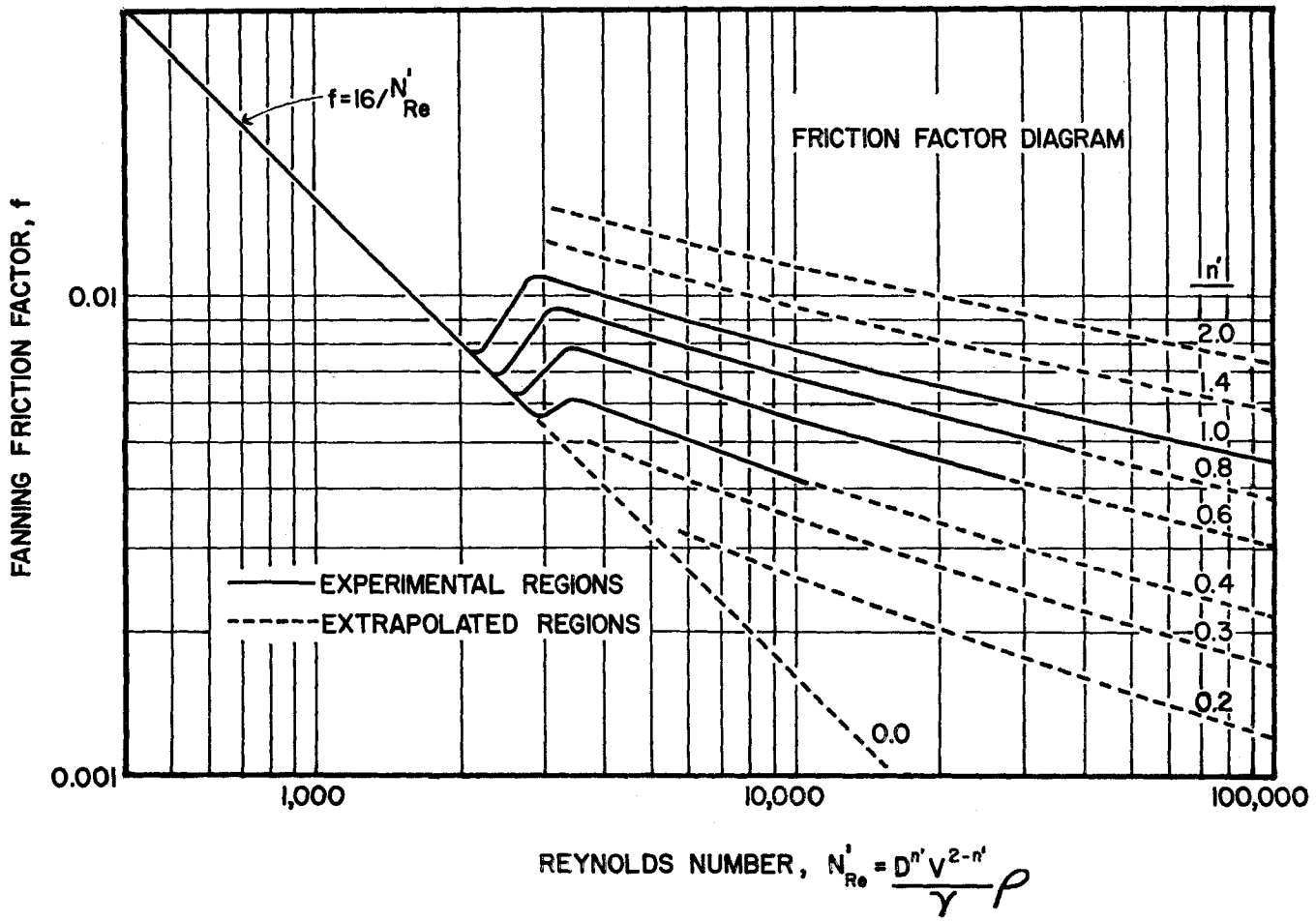

Fig. 12. Final friction factor design chart for Newtonian and non-Newtonian fluids.

(29) or now Equation (45) will be applicable to nonpower-law fluids, provided that the fluid-property parameters are evaluated at the wall shear stress. Perhaps the best way to test this hypothesis and concomitantly to use the nonpower-law data to check the proposed A_{1_n} and C_n' functions is to compare the experimental friction factor for the nonpower-law fluids with those predicted by Equation (45). By means of experimental Reynolds numbers and the appropriate flow-behavior indexes, Equation (45) has been solved for the friction factor corresponding to each turbulent non-Newtonian test made during this investigation. By including in such a comparison the power-law fluids on which A_{1_n} and C_n' were based, the accuracy of Equation (45) may be investigated. Figure 11 is a plot of $f_{expt'l.}$ vs. $f_{pred.}$ showing these results for the non-Newtonian tests only.

Excellent agreement is found between the predicted and experimental friction factors. The points of Figure 11 cover a range of the flow-behavior index from 0.36 to 0.73 and of the Reynolds number from 2,900 to 36,000. (The highest Reynolds numbers correspond also to the highest values of n'.) Results for the nonpower-law fluids (primarily the clay suspensions) show equal agreement with the predicted friction factors, as do the power-law fluids on the basis of which the correlating equation was developed. Hence it is proved that, as predicted, Equation (45) is applicable to nonpower-law as well as power-law systems, provided the fluid-property parameters are evaluated at the existing wall shear stress. Also the conformity of the nonpower-law fluids to Equation (45) serves serves indirectly to support the validity of the proposed A_{1_n} and C_n' functions. The data of Figure 11 are grouped into three ranges of n' to illustrate the absence of an effect of the flow-behavior index on the degree of agreement. The 146 points shown in Figure 11 represent all the turbulent non-Newtonian experiments of this investigation. The maximum deviation of an experimental friction factor from the value predicted by Equation (45) is 8.5%, and the mean absolute deviation is 1.9%. Sixty-nine per cent of the deviations lie within the standard deviation of 2.4%, an indication that the deviations of the experimental points from those predicted conform to a statistically normal distribution.

The main objective of this study is the friction-factor–Reynolds-number correlation given by Equation (45). Since this equation cannot be solved for f explicitly, a graphical presentation of the equation will be found convenient for future use. Figure 12 is a friction-factor plot based on Equation (45) in the turbulent region. The solid lines of this figure indicate the region in which experimental data were taken, whereas the dashed lines represent modest extrapolations by use of Equation (45).

DISCUSSION

Friction-Factor Correlation

The validity of the theoretical relationship developed in this work between the friction factor and the generalized Reynolds number has been established for polymeric solutions, solid-liquid suspensions, power-law, and nonpower-law fluids alike. Equation (45) has been shown to agree very well with the experimental data covering a range of flow-behavior indexes from 0.36 to 1.0. The extrapolations of Figure 12 extend this region of n' to from 0.2 to 2.0, and it is believed that such moderate extrapolations are entirely permissible. Caution should be observed, however, in extrapolating Equation (45) to values of n' greatly removed from the experimental range. For very highly dilatant fluids the assumption of a negligible thickness of the laminar sublayer which is incorporated into Equation (7) may fail. On the other hand, when n' becomes extremely small, for example 0.001, the C_n' function becomes a significant

part of the quantity $(1/f)^{\frac{1}{2}}$ and may well require more accurate evaluation than can be obtained by extrapolation according to Equation (44). Actually however it is to be expected that turbulent-flow problems involving flow-behavior indexes outside the range of Figure 12 will be exceedingly rare, and therefore that Figure 12 will be adequate in nearly all practical cases. Extrapolations to Reynolds numbers higher than the experimental range at a given value of n' should be quite permissible, since all the assumptions involved in the theoretical development of Equation (45) become even more valid as the Reynolds number is increased.

For the non-Newtonian systems studied in this investigation (n' less than unity) the onset of turbulence always occurred at Reynolds numbers slightly greater than those for Newtonian fluids. Furthermore the data showed some evidence that the Reynolds number corresponding to the onset of turbulence increases slowly with decreasing values of the flow-behavior index. For example with an n' of 0.726 Figure 7 indicates the start of the transition region at a Reynolds number of about 2,700, whereas for an n' of 0.38 the onset of turbulence was observed at a Reynolds number of about 3,100. Unfortunately the effect was not clear-cut, since the experimental data close to the onset of turbulence exhibited sufficient scatter to prohibit a precise definition of the transition region. Of necessity the transition-region portions of the friction-factor curves of Figure 12 were located somewhat arbitrarily but in general accordance with the experimental observations.

An interesting point arises regarding the case of ultimate pseudoplasticity ($n' = 0$). It was reasoned earlier that laminar- and turbulent-velocity profiles for this situation would be identical and that as a result the turbulent friction-factor–Reynolds-number correlation would simply be an extension of the laminar relationship. In view of the apparent increase of the critical Reynolds number with decreasing n', indicated by the present results, however, a question arises as to whether or not a turbulent-flow condition could ever be attained for this case. With a perfectly flat laminar-velocity profile the flow instability frequently attributed to the influence of a velocity gradient is absent. Everywhere within a tube except at the wall itself the stability parameter of Rouse (*14*) would be zero, an indication of complete stability. Directly at the tube wall the stability parameter becomes indeterminate. If turbulence were to begin just at the tube wall, which in itself is a questionable notion, it is not clear that propagation would ensue throughout the tube.

An additional non-Newtonian system heretofore unmentioned was studied which did not behave in the same manner as the other experimental fluids. Figure 13 shows a series of friction-factor measurements taken with a 0.3% aqueous solution of carboxymethycellulose (CMC). The friction factor here follows much more closely an extension of the laminar line than do the data for the other fluids, and a pronounced diameter effect is evident. These observations plus others that will not be pursued here all indicated that the abnormalities manifested by the CMC data are the result of some type of pseudostable laminar- or transitional-flow condition, and that fully developed turbulent-flow was never achieved with these fluids. On the other hand the flow situation obviously deviated from purely laminar motion. It would appear that CMC solutions possess some abnormal ability to suppress the formation and propagation of turbulence. The physical mechanisms responsible for the peculiar behavior of these fluids are not known at the present time, although several possible explanations may be cited (*3*), of which viscoelasticity appears to be the most probable. That the CMC system represents the abnormal non-Newtonian case seems certain from a consideration of other available turbulent data for a variety of fluid systems (*11*). In no instance have prior data been reported which resemble the CMC results of this investigation; in all cases a definite break from laminar flow occurred at values of the generalized Reynolds number only slightly greater than 2,100, as in the present study. When one notes that the prior-art data on well-developed turbulent flow are entirely for slurries, it appears that the correlation presented here is of primary value for such systems. Accordingly this correlation is recommended for use with slurries, but it may also be used for polymeric material provided at least one experimental measurement, under turbulent conditions, is available to determine whether the fluid in question falls into the same category as slurries and the Carbopol (polymeric) solution or into the category of CMC. If such a single measurement is not available, the present design chart may still be used as the best available approximation, since it will always be either correct or, if in error, conservative.

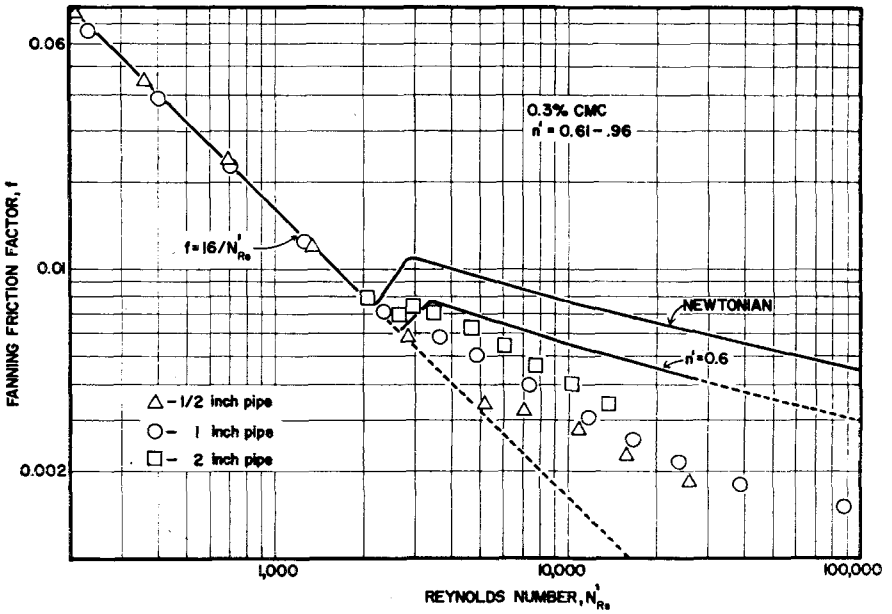

Fig. 13. Friction factor results for anomalous fluid.

The simplest explanation for the observed difference between the behavior of CMC on the one hand and of Carbopol and slurries on the other is that one or more additional and as yet undefined physical properties are of significance in the case of CMC and other polymer solutions which may later be shown to fall into the same category as CMC. If one were to develop a design chart such as is given in Figure 12 by using CMC solutions of various concentrations, the results would obviously be different from those of Figure 12, even though they might be self-consistent. Since the magnitudes of the unknown but necessary physical properties are not available, such a chart would be of little or no value for use with other fluids; it would obviously be inapplicable to slurries, but more important it would also be inapplicable to other fluids of the general nature of CMC unless they fortuitously possessed exactly the same value of the unknown parameters as does CMC. In view of this rather small probability such a design chart would not be of proved utility except for use with CMC. It is unfortunate that this situation has arisen in another study (*16*) in which CMC was the only fluid used having a flow-behavior index below 0.70. Since the difference between the friction factors for a Newtonian fluid and one

with an n' of 0.70 is less than 25% (Figure 12), while Shaver's (*16*) accuracy was stated to be only ± 12%, it is clear that the one part of Shaver's study which possibly does not contain complications, owing to CMC-like behavior, does not serve to predict the trend of friction factors as a function of n' with better than order-of-magnitude accuracy.

Prior-Art Correlation Methods

Earlier workers have almost unanimously adopted the apparent thesis (although not always stated explicitly) that the shear rates occurring under turbulent conditions are high enough to effect constancy of viscosity and permit correlation of pressure-loss–flow-rate data by standard Newtonian procedures. In essence such studies were not concerned at all with the actual turbulent behavior of non-Newtonian fluids but simply the turbulent behavior of Newtonian systems, which under different circumstances would exhibit non-Newtonian characteristics. The main difference between several approaches proposed in the past has been in defining what value should be used as the constant viscosity. The three primary approaches of the prior art have been based on the use of the viscosity of the dispersion medium (*2*), a limiting viscosity at infinite shear (*1, 21, 22*), and a turbulent viscosity established from sample pressure-loss measurements taken on the given fluid under actual turbulent conditions (*1, 19*).

Portions of the data from the present investigation have been treated according to these prior-art schemes to test the reliability of these three procedures (*3*). The turbulent viscosities were found to be 1.3 to 5.3 times larger than the limiting viscosities at infinite shear and from three to fourteen times as large as the viscosity of the dispersion medium. Obviously both of the first two design methods are of very limited values. The turbulent viscosities were also found to be variables rather than constants as suggested by the prior art. In fact they varied as much as threefold over a fivefold range of Reynolds numbers.

The most extensive correlation of early data treated all the consistent non-Newtonian data then available in the literature (*11*). The results were presented as a plot of friction factor vs. N_{Re}'. This plot showed the end of the stable, laminar flow region occurring at a Reynolds number of 2,100 to 3,000, followed by a broad region extending to $N_{Re}' = 70{,}000$, in which the friction factor was nearly constant. It is very probable that most of the fluids involved were changing from non-Newtonian to Newtonian character at the shear stresses prevalent in the apparent transition region and that this rheological change

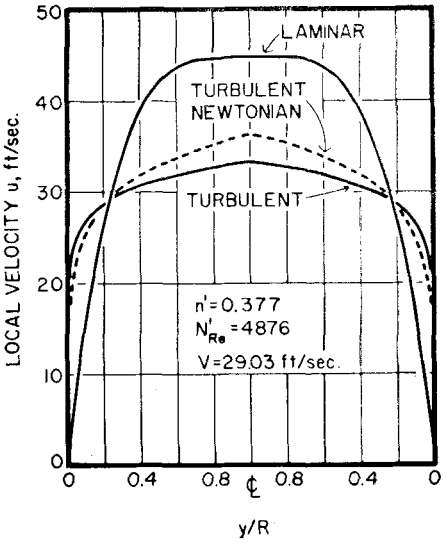

Fig. 14. Typical predicted velocity profiles. All curves are calculated for the same average velocity.

was responsible for the constancy of the friction factor at Reynolds numbers above 2,100 rather than an actual transition phenomenon. The results of the present investigation confirm this premise. Figure 12 illustrates that for fluids with flow-behavior indexes that increase from some low value toward unity, results identical to those observed by Metzner and Reed are to be expected. Thus while their method of correlation represented a considerable improvement over the methods discussed, limitations of the available data prevented development of a truly precise design procedure.

Comprehensive discussions of other (less important) early studies of turbulence in non-Newtonian systems are available in references *3* and *11*.

Velocity Profiles

If one assumes the g_1 function to be zero, it was predicted from theory that the turbulent-velocity defect for power-law non-Newtonians is given by Equation (34). When Equations (34) and (45) are combined, this predicted velocity-defect law becomes

$$\frac{U_m - u}{u^*} = 5.66(n')^{0.25} \log \frac{R}{y} \quad (46)$$

The integrated form of the velocity-defect law corresponding to Equation (40) becomes by similar substitution

$$\frac{U_m - V}{u^*} = P_n = 3.686(n')^{0.25} \quad (47)$$

Although Equations (46) and (47) both indicate the flattening influence of a decreasing flow-behavior index on the turbulent-velocity profile, this effect may be appreciated more fully by an examination of the velocity profile itself rather than the velocity defect. Figure 14 shows a predicted turbulent-velocity profile based on a set of conditions representing one of the actual experimental points. Such a profile is readily calculated by using Equations (8), (45), (46), and (47). Included for comparison are the laminar-velocity profile for a fluid having the same properties and a turbulent Newtonian profile corresponding to the same Reynolds number and mean velocity. The pronounced flattening of the laminar profile on transition from laminar to turbulent flow owing to the turbulent transfer of momentum is obvious at once. It is worth noting that although pseudoplastic fluids have laminar profiles which are flat relative to the parabolic velocity distribution characteristic of Newtonian laminar motion, the laminar profile for $n' = 0.377$ is still considerably less flat than the turbulent Newtonian profile.

It has been shown that for power-law fluids the velocity profiles may also be expressed in terms of generalized u^+ and y^+ functions. Equation (36) expresses the relationship between these dimensionless quantities within the turbulent core. When the general A_n and B_n functions are replaced with their proposed functional forms, Equation (36) becomes

$$u^+ = \frac{5.66}{(n')^{.75}} \log y^+ - \frac{0.40}{(n')^{1.2}}$$

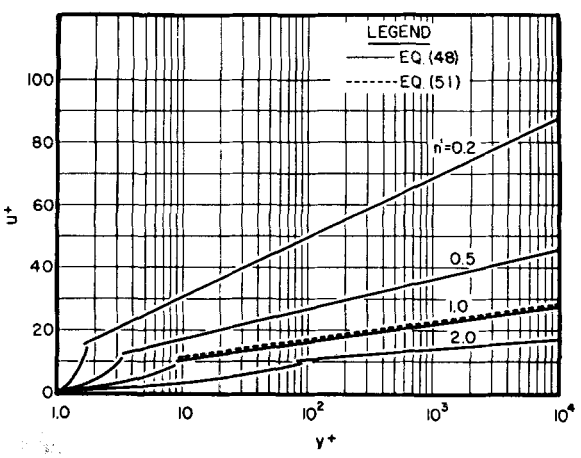

Fig. 15. Generalized ($u^+ - y^+$) velocity profile plot for non-Newtonian as well as Newtonian fluids.

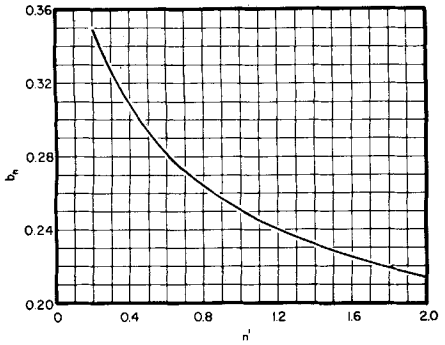

Fig. 16. The b_n function in the relation

$$f = \frac{a_n}{(N_{Re}')^{b_n}}.$$

$$+ \frac{2.458}{(n')^{.75}}\left[1.960 + 1.255n' - 1.628n' \log\left(3 + \frac{1}{n'}\right)\right] \quad (48)$$

With any given value of n' Equation (48) simplifies greatly and loses its prodigious appearance. For example for the Newtonian case Equation (48) reduces to

$$u^+ = 5.66 \log y^+ + 5.1 \quad (49)$$

Direct velocity-profile measurements on Newtonian fluids have yielded the equations (*15*)

$$\frac{U_m - u}{u^*} = 5.75 \log \frac{R}{y} \quad (50)$$

$$u^+ = 5.75 \log y^+ + 5.5 \quad (51)$$

The differences between Equations (49) and (51) and Equations (46) and (48) for the Newtonian case are small. The slight discrepancies in the comparative coefficients arise from the fact that frictional pressure-loss measurements have been used to establish the coefficients in Equations (46) through (49), whereas direct velocity-profile measurements were used in the case of Equations (50) and (51). Any small real differences here are perhaps ascribable to slight inaccuracies encountered during the development, such as the neglect of the laminar sublayer when one is integrating for the mean velocity or the slight inaccuracy of the velocity-defect equation at the center line. Again it is noted that Equations (46) and (48) cannot be perfect, since they do not predict a zero shear rate at the center line of the tube. However in view of the adequacy and widespread acceptance of the corresponding Newtonian Equations (50) and (51), which suffer the same objection, this discrepancy is not considered to constitute a major inconsistency under all conditions. However careful examination of Figure 14 shows that the error introduced appears to increase with decreasing values of n'; that is, the region near the center line in which

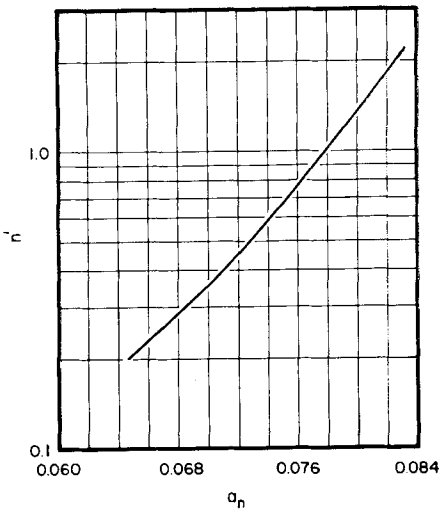

Fig. 17. The a_n function in the relation

$$f = \frac{a_n}{(N_{Re}')^{b_n}}.$$

the turbulent equations predict a steeper profile rather than one which is flatter than the corresponding laminar profile has been increased in breadth for the non-Newtonian case. This makes the theoretically predicted turbulent-velocity profiles for non-Newtonian fluids an extremely tentative proposition until checked by direct experimental measurements. The only available experimental velocity profiles appear to be in the unpublished thesis of Shaver (*16*). Since it is believed that his data may possibly be influenced by unmeasured complications owing to fluid elasticity or another similar effect, there appear to be no experimental measurements of proved applicability with which the present predictions may be verified or rejected at this time.

Equation (48) is shown plotted for several values of the flow-behavior index in Figure 15. A plot of Equation (51) is also included for comparison. Within the laminar sublayer Equation (39) becomes valid replacing Equation (36). Curves representing Equation (39) for the corresponding values of n' are also shown in Figure 15. It is likely that some type of buffer or transition region separates and causes a gradual merging of the laminar sublayer and turbulent core rather than the abrupt transition indicated by the intersections of Figure 15. Velocity-profile measurements with Newtonian fluids have certainly indicated the presence of such a buffer region (*5*, *15*). However the question of the existence and extent of a buffer region with non-Newtonian fluids must await suitable measurements on velocity profiles themselves.

Blasius Type of Approximation

It was indicated earlier that Equation (42), a simple expression resembling the equation proposed by Blasius for Newtonian liquids, might be used for non-Newtonian fluids to provide an approximation of the friction factor within a limited range of Reynolds numbers. Figures 16 and 17 post the best values of b_n and a_n over the Reynolds number range from 3,000 to 100,000 as obtained by fitting straight lines to the curves of Figure 12. Figure 18 shows the turbulent friction-factor lines predicted by Equation (42), based on the smoothed a_n and b_n functions as given in Figures 16 and 17 respectively. For comparison the corresponding curves predicted by Equation (45) are included.

Contraction Effects

When a fluid is allowed to flow through a sharp-edged entrance or sudden contraction, a finite length of flow path is required thereafter before a fully developed velocity profile is attained. To trace the extent of entrance or contraction effects a sharp-edged contraction from 1½- to ½-in. standard pipe was installed at the entrance to the calming section of the ½-in. pipe. Three pressure taps were placed in the calming section downstream from the contraction, so

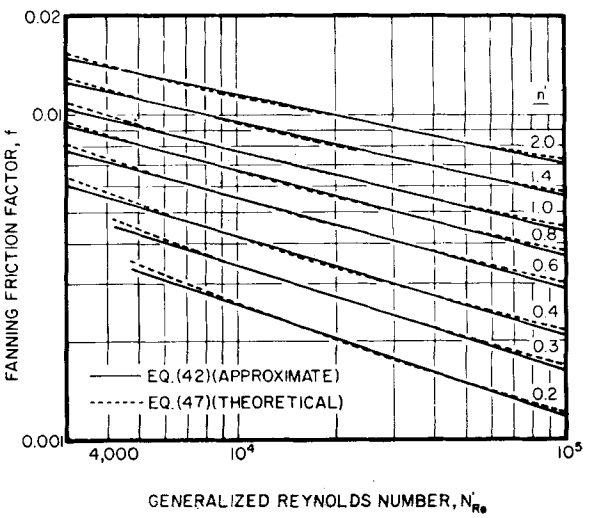

Fig. 18. Comparison of approximate and theoretical equations for the friction factor.

that the pressure gradient might be traced back from the test section to within 5.6 diam. of the point of contraction.

Figure 19 illustrates a typical pressure gradient following the contraction, when laminar flow prevailed. The excessive pressure loss, immediatley evident near the contraction, appears to be dissipated completely at about 45 diam. downstream, after which a linear pressure gradient was established. There was some indication that the distance over which the contraction influence was felt increased slightly with increasing velocity or Reynolds numbers, but the data were inadequate to establish any quantitative relationship. In no case however did the laminar entrance length extend appreciably beyond the 53 diam. allowed in this work as a calming section.

Owing to eddy momentum transport it is to be expected that turbulent entrance lengths will be considerably less than for the laminar case at corresponding Reynolds numbers. Experimental data have verified this hypothesis. The entrance lengths under turbulent conditions were so short that their determination was almost impossible. Generally it can be said that all observed turbulent entrance lengths were less than 15 diam. and appeared to be independent of the velocity or Reynolds number. These entrance length results qualitatively agree with similar Newtonian measurements and are of comparable magnitude or somewhat shorter. Since the non-Newtonian velocity profiles for fluids having an n' of less than unity are always less sharp than in the corresponding Newtonian case, it appears reasonable from a theoretical point of view that a shorter distance should be required to establish the final profile, other factors being constant. It should be noted that entrance lengths determined from excess pressure losses in the region of a contraction are generally smaller than those required to develop completely the velocity profile, since the final velocity distribution is attained earlier in the vicinity of the wall, which determines the pressure gradient, than at the center line of the tube.

By extrapolating the excess pressure curves back to zero length, as is shown in Figure 19, it is possible to arrive at the excess pressure loss which is dissipated within the smaller pipe. Such an excess pressure loss is not equivalent to the total contraction loss, since it does not include the portions of the kinetic energy change and additional fluid friction which take place in the larger pipe prior to the point of contraction. Figure 20 is a plot of the experimentally determined laminar excess pressure losses including kinetic energy effects determined in this manner as a function of the mean velocity. It can be seen that all the data are correlated quite well by a line

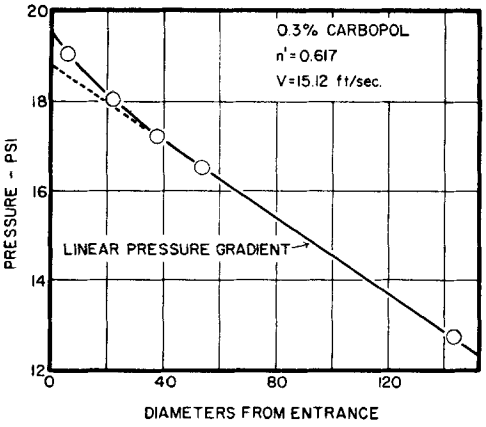

Fig. 19. Typical pressure gradient downstream from an abrupt contraction.

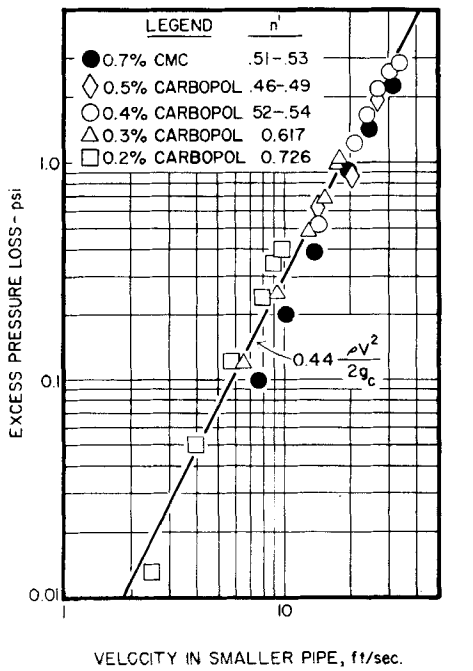

Fig. 20. Laminar contraction losses.

corresponding to 0.44 velocity heads and that no significant effect of the flow-behavior index is apparent. No contraction losses were obtained for the tests corresponding to turbulent conditions, since the accompanying entrance lengths were too short to permit the necessary extrapolation with even a moderate degree of accuracy. However there were very strong indications that turbulent contraction losses correspond to considerably fewer velocity heads than do laminar contraction losses, which is in qualitative agreement with the finding of Weltmann and Keller (*21*).

McMillen (*8*) measured laminar-contraction pressure losses in exactly the same manner as was used in the present study and following contractions comparable to those used here. His results showed losses from four to ten velocity heads and indicated that the losses increased with the 1.5 power of the mean velocity rather than as the square. The large discrepancy between such findings and the others mentioned is obvious and possibly is due to the high viscoelasticity of McMillen's fluid.

When rheological properties were calculated from measurements with the capillary-tube viscometer, an entrance correction of 1.5 $\rho V^2/g_c$ was arbitrarily assumed for lack of more accurately defined procedures. For the vast majority of data this correction was entirely negligible. Only at the highest shear rates did the correction term become appreciable. Employing capillary tubes of several diameters so that the linear velocities were different at the same shear stress made it possible to examine the appropriateness of the assumed entrance correction. Nearly all the data indicated that the correction of 1.5 $\rho V^2/g_c$ was too large. Although the actual entrance losses could not be established precisely from these observations, it appeared that a correction closer to 1.0 $\rho V^2/g_c$ or the Newtonian correction of 1.12 $\rho V^2/g_c$ would have been nearer to the fact for all the fluids of this investigation. Such a conclusion supports the findings of Toms (*17*) and Weltmann and Keller (*21*). This capillary correction includes the entire kinetic energy and frictional effects encountered at an essentially infinite reduction in cross section, which certainly should be larger than those at the 2.56:1-diam. reduction employed as the pipeline contraction. Consequently the laminar-contraction losses for the pipeline contraction should be expected to be less than two velocity heads, which again agrees qualitatively with the experimental findings after allowance is made for upstream losses in the pipeline apparatus.

SUMMARY AND CONCLUSIONS

The present work represents the first theoretical attack in the area of turbulent non-Newtonian flow and has yielded a completely new concept of the attending relationship between the pressure loss and average flow rate based solely on fundamental fluid properties. The turbulent resistance law resulting from this analysis resembles the well-known equation of von Karman for Newtonian fluids but represents a generalization thereof which is applicable to Newtonian and non-Newtonian fluid systems alike, irrespective of any arbitrary rheological classifications. To be rigorous the relationship is restricted to nonelastic, time-independent fluids, which represent the simplest and fortunately the most common case of flow behavior. The latter restriction of time independency however, is of little engineering importance, since it is probable that design calculations with such fluids would be based on the limiting cases of zero and infinite times of shear, representing

start-up and steady state conditions. These limiting cases may be treated individually as if time effects were absent.

The friction-factor relationship given by the theoretical analysis is

$$\sqrt{\frac{1}{f}} = A_{1n} \log [N_{Re}'(f)^{1-n'/2}] + C_n'$$

The A_{1n} and C_n' functions required experimental determination, just as in the case of earlier theoretical analyses developed for the simpler special case of Newtonian behavior.

All the fully turbulent experimental data supported the validity of the theoretical analysis. The A_{1n} and C_n' functions were established primarily from data taken with polymeric solutions. Subsequent comparison between predicted and experimental friction factors for clay suspensions, however, showed equally good agreement. The final equation

$$\sqrt{1/f} = \frac{4.0}{(n')^{0.75}} \log [N_{Re}'f^{1-n'/2}] - \frac{0.4}{(n')^{1.2}}$$

correlated all the turbulent non-Newtonian data for both the slurries and the nonelastic gels (some 146 points) with a mean deviation of 1.9%. Correlation of these data by the empirical prior-art methods showed much poorer agreement and indicated that the prior-art procedures become progressively worse as the intensity of the non-Newtonian characteristics increase. For fluid systems with flow-behavior indexes that are functions of the shear stress it has been shown that n' should be evaluated at the existing wall shear stress for use in the proposed relationship. A friction-factor expression approximating the theoretical equation for Reynolds numbers less than 100,000, but which expresses the friction factor explicitly, has also been developed.

Transition from laminar to turbulent flow with non-Newtonian systems was found to take place within a Reynolds number range comparable to the extent of the Newtonian transition region. The lower critical Reynolds number corresponding to the onset of turbulence appeared to increase slightly with decreasing values of the flow-behavior index. At n' equal to 0.38 the onset of turbulence was observed at a Reynolds number of about 3,100.

The theoretical analysis of the present work has permitted the prediction of non-Newtonian turbulent velocity profiles, for which no published literature exists. Although no velocity profiles were actually measured, comparison of this work with the accepted Newtonian relationships indicates that these predictions should be reasonably valid. Generalizations of familiar u^+ and y^+ velocity-profile parameters have been proposed which extend their utility to non-Newtonian systems.

Pressure-loss measurements taken near a sudden contraction have provided information, although somewhat limited, on the tube lengths over which an entrance effect is observable with non-Newtonian fluids and the magnitude of entrance or contraction losses.

These conclusions are based on data taken with one type of polymeric gel and with slurries. Preliminary measurements on another gel system showed turbulence to be strongly suppressed, perhaps owing to elasticity effects, which have not been considered in the present analysis. The present results may however be used as an approximation for such fluids; while the predicted friction factors may be in error, they will be conservative.

The need for further work lies primarily in characterization of such more complex gels and extension of the present approach to such systems, measurement of velocity profiles to verify the theoretical predictions made herein, and application of this knowledge of the mechanics of turbulence in non-Newtonian systems to problems in areas such as fluid agitation and heat and mass transfer.

ACKNOWLEDGMENT

Sincere gratitude is extended to the Texas Company, the United States Army Office of Ordnance Research, and the United States Air Force Bureau of Scientific Research, whose sponsorship made this work possible.

NOTATION

a_n = dimensionless function of flow-behavior index for Blasius type of approximation, defined by Equation (42)

A_n = dimensionless function of flow-behavior index (constant at any given value of n)

A_{1n} = dimensionless function of flow-behavior index

b_n = dimensionless function of flow-behavior index for Blasius type of approximation, defined by Equation (42)

B_n = dimensionless function of flow-behavior index

C_n = dimensionless function of flow-behavior index, defined by Equation (21)

C_n' = dimensionless function of flow-behavior index, defined by Equation (29)

D = internal diameter of pipe or tube

e_n = dimensionless function of flow-behavior index for assumption of strict similarity

E_n = dimensionless function of flow-behavior index

f = Fanning friction factor (dimensionless), also used to designate an unspecified function when followed by series of variables in parentheses

g_c = dimensional conversion factor, 32.17 (lb.-mass/lb.-force) (ft./sec.^{2})

g_1 = general function of ξ and the flow-behavior index defined by Equation (19)

k = turbulent constant appearing in theoretical relationships for Newtonian fluids

K = fluid consistency index defined by Equation (1)

K' = fluid consistency index defined by Equation (24)

L = length of pipe or tube

n = flow-behavior index (dimensionless), defined by Equation (1)

n' = flow-behavior index (dimensionless), defined by Equation (23)

N_{Re} = conventional Reynolds number (dimensionless), $DV\rho/\mu$

N_{Re}' = generalized Reynolds number (dimensionless), defined by Equation (28)

N_{Re}° = Reynolds number (dimensionless), defined by Equation (22)

P_n = dimensionless function of flow-behavior index, defined by Equation (7)

ΔP = pressure drop, $\Delta P/L$, pressure gradient

Q = volumetric flow rate

r = radial distance from center of tube

R = internal radius of pipe or tube

u = local velocity at r (or y)

u^* = friction or shear velocity, equal to $\sqrt{\tau_w/\rho}$

u^+ = dimensionless velocity-profile parameter, defined by Equation (37)

U_m = maximum (center line) linear velocity in tube

V = mean linear velocity

y = distance from tube wall, equal to $(R - r)$

y^+ = dimensionless velocity-profile parameter, defined by Equation (38)

Z = dimensionless group defined by Equation (4)

Greek Letters

δ = value of y at the intersection of the laminar sublayer and transition zone

λ = value of y at the intersection of the transition zone and the turbulent core

μ = viscosity of a Newtonian fluid

ξ = dimensionless location parameter, equal to y/R

ξ_1 = value of ξ slightly larger than λ/R

ρ = density

τ = shear stress, equal to $(r\ \Delta P/2L)$ within round tube

τ_w = shear stress at inner wall of tube $(D\ \Delta P/4L)$

γ = grouping of terms forming denominator of the generalized Reynolds number, $\gamma = g_c K' 8^{n'-1}$

LITERATURE CITED

1. Alves, G. E., D. F. Boucher, and R. L. Pigford, *Chem. Eng. Progr.*, **48**, 385 (1952).
2. Caldwell, D. H., and H. E. Babbitt, *Trans. Am. Inst. Chem. Engrs.*, **37**, 237 (1941); *Ind. Eng. Chem.*, **33**, 249 (1941).
3. Dodge, D. W., Ph.D. thesis, Univ. of Delaware, Newark, Delaware (1957).
4. Durand, W. F., "Aerodynamic Theory," III, 127, 142, Julius Springer, Berlin (1935).
5. Hunsaker, J. C., and B. G. Rightmire, "Engineering Applications of Fluid Mechanics," McGraw-Hill, New York (1947).
6. Knudsen, J. G., and D. L. Katz, *Eng. Research Bull.* **37**, Univ. of Mich. Press, Ann Arbor, Michigan (1954).
7. Krieger, I. M., and S. H. Maron, *J. Appl. Phys.*, **23**, 147 (1952).
8. McMillen, E. L., *Chem. Eng. Progr.*, **44**, 537 (1948).
9. Metzner, A. B., "Advances in Chemical Engineering," vol. I, Academic Press, New York (1956).
10. ———, *Ind. Eng. Chem.*, **49**, 1429 (1957).
11. ———, and J. C. Reed, *A.I.Ch.E. Journal*, **1**, 434 (1955).
12. Millikan, C. B., "Proc. Fifth Int. Cong. for Appl. Mechanics," 386, John Wiley and Sons, (1939).
13. Rabinowitsch, B., *Z. physik. Chem.*, **A145**, 1 (1929).
14. Rouse, Hunter, "Elementary Mechanics of Fluids," John Wiley and Sons, Inc., New York (1946).
15. Schlichting, Hermann, "Boundary Layer Theory," McGraw-Hill Book Co., New York (1955).
16. Shaver, R. G., Sc.D. thesis, Mass. Inst. Technol., Cambridge, Massachusetts (1957).
17. Toms, B. A., "Proc. 1st Int. Rheolog. Cong., Holland," II, 135 (1948).
18. von Karman, Th., *Nachr. Ges. Wiss. Gottingen, Math. physik. Kl.*, 58 (1930), and "Proc. of 3rd Int. Cong. of Appl. Mechs., Stockholm, Pt. 1," 85 (1930); also *Natl. Advisory Comm. Aeronaut., Tech. Mem. No.* 611, Washington, D. C. (1931).
19. Ward, H. C., Ph.D. thesis, Georgia Inst. of Technol., Atlanta, Georgia (1952).
20. Weltmann, R. N., *Natl. Advisory Comm. Aeronaut., Tech. Note* 3397 (1955); *Ind. Eng. Chem.*, **48**, 386 (1956).
21. ———, and T. A. Keller, *Natl. Advisory Comm. Aeronaut., Tech. Note* 3889 (1957).
22. Winding, C. C., G. P. Baumann, and W. L. Kranich, *Chem. Eng. Progr.*, **43**, 527, 613 (1947).

Manuscript received February 4, 1958; revision received July 3, 1958; paper accepted July 7, 1958. Paper presented at A.I.Ch.E. Chicago meeting.

Characteristics of Transition Flow Between Parallel Plates

G. A. WHAN and R. R. ROTHFUS

Carnegie Institute of Technology, Pittsburgh, Pennsylvania

Measurements of pressure drop and mean local fluid velocities have been made in a smooth rectangular duct of large aspect ratio. Data have been taken on the steady, isothermal flow of water at room temperature in the viscous, transition, and lower turbulent ranges of flow. Impact probes were installed in the center of the stream, where flow between infinitely broad parallel plates was closely approximated. The limits of the transition range are discussed, and mean local fluid velocities are correlated. Comparison is made with transitional behavior in smooth tubes.

The present investigation was undertaken to gain information about the characteristics of steady, isothermal, fluid flow between smooth, parallel, flat plates. Attention was centered on the region of laminar-turbulent transition, although data were obtained in the viscous and lower turbulent ranges as well. The test fluid was water at room temperature flowing at Reynolds numbers between 865 and 40,190. Measurements of temporal mean local fluid velocities were made by means of a calibrated impact probe, and these data were supplemented by corresponding measurements of the pressure drop caused by fluid friction. Forty-six velocity profiles were obtained to furnish a comprehensive picture of their dependence on the Reynolds number.

Since it was impossible to deal with infinitely broad plates, these were approximated by the long sides of a 0.70- by 14-in. rectangular conduit, 20 ft. in horizontal length, formed from brass plates and equipped with a bell-shaped entrance. The 20:1 aspect ratio of the duct permitted the experimental data to be compared with published information in the fully turbulent range.

Several investigations, such as those of Laufer (*3*), Skinner (*10*), and Wattendorf and Kuethe (*13*), have been made to determine the velocity distribution for air flowing in fully turbulent motion between parallel plates. More recently Sage and coworkers (*2, 4*) have obtained several excellent velocity profiles in the lower turbulent region. Their apparatus was much like that used in the present experiments. Schlinger and Sage (*8*) have presented a correlation of available velocity data for parallel plates. Using the date of Sage and coworkers as their basis, Rothfus and Monrad (*6*) have developed a means of correlating parallel-plate velocity profiles with those obtained in smooth tubes under fully turbulent conditions. Rothfus and coworkers (*5*) have presented simplified methods of calculating velocity profiles and pressure drops based on the Rothfus and Monrad correlation. The fully turbulent range of flow can therefore be handled reasonably well with respect to fluid friction and the distribution of mean local velocities, provided the calming length is sufficient to make entrance effects negligible.

In the fully viscous range of flow the Navier-Stokes equations of motion can

G. A. Whan is at the University of New Mexico, Albuquerque, New Mexico.